TITLE PAGE

TYPE OF ARTICLE: Major Article

MANUSCRIPT TITLE: Repetitive aerosol exposure promotes cavitary tuberculosis and enables screening for targeted inhibitors of extensive lung destruction.

RUNNING TITLE: Repetitive aerosol exposure to model cavitary tuberculosis.

LIST OF AUTHORS: Michael E. Urbanowski[+, 1], Elizabeth A. Ihms[+, 1, 2], Kristina Bigelow[1], André Kübler[3], Paul T. Elkington[4, 5], William R. Bishai[1,*].

AUTHOR AFFILITATIONS:

Michael E. Urbanowski	+	The authors contributed equally to this work.
	1.	Center for Tuberculosis Research, Department of Medicine, The Johns Hopkins University School of Medicine, Baltimore, Maryland, USA.
Elizabeth A. Ihms	+	The authors contributed equally to this work.
	1.	Center for Tuberculosis Research, Department of Medicine, The Johns Hopkins University School of Medicine, Baltimore, Maryland, USA.
	2.	Department of Molecular and Comparative Pathobiology, the Johns Hopkins University School of Medicine, Baltimore, Maryland, USA.
Kristina Bigelow	1.	Center for Tuberculosis Research, Department of Medicine,

The Johns Hopkins University School of Medicine, Baltimore, Maryland, USA.

André Kübler   3. Queen's Hospital, Barking, Havering and Redbridge University Hospital NHS Trust, Romford, Essex, RM7 0AG, UK.

Paul T. Elkington   5. NIHR Biomedical Research Centre, Clinical and Experimental Sciences Academic Unit, Faculty of Medicine, University of Southampton, Southampton, UK.

6. Institute for Life Sciences, University of Southampton, UK

William R. Bishai   1. Center for Tuberculosis Research, Department of Medicine, The Johns Hopkins University School of Medicine, Baltimore, Maryland, USA.

*   The corresponding author. 1550 Orleans St. Rm 108, Baltimore MD 21231 (wbishai@jhmi.edu)

40 WORD SUMMARY: Repetitive aerosol exposure in the rabbit TB model generated a greater number of cavities and increased lung damage than when the same inoculum was given once. The model was used to test an anti-MMP1 drug, cipemastat, as a host-directed therapy.

FOOTNOTE PAGE

CONFLICT OF INTEREST STATEMENTS:

Michael E. Urbanowski | No conflicts of interest.

Elizabeth A. Ihms | No conflicts of interest.

Kristina Bigelow | No conflicts of interest.

André Kübler | No conflicts of interest.

Paul T. Elkington | No conflicts of interest.

William R. Bishai | No conflicts of interest.

CONFERENCE PRESENTATIONS:

(1) Keystone Symposia on Molecular and Cellular Biology: New Development in Our Basic

Understanding of Tuberculosis. Vancouver, British Columbia, Canada. January 14-18,

2017. Poster Number: 3053

ABSTRACT

Background.   Cavitation is a serious consequence of tuberculosis. We tested the hypothesis that repetitive exposure to the same total bacterial burden of *Mtb* drives greater lung destruction than a single exposure. We also tested whether inhibition of endogenous MMP1 may inhibit cavitation during TB.

Methods. Over a three weeks interval we infected rabbits with either 5 aerosols of 500 CFU of *Mtb* or a single aerosol of 2500 CFU plus four sham aerosols. We administered the MMP1 inhibitor cipemastat (100 mg/kg daily) from week 5-10 to a subset of the animals.

Results. Repetitive aerosol infection produced greater lung inflammation and more cavities than a single aerosol infection of the same bacterial burden (75% of animals versus 25%). Necropsies confirmed greater lung pathology in repetitively exposed animals. For cipemastat-treated animals there was no significant difference in cavity counts, cavity volume, or disease severity compared to controls.

Conclusions. Our data show that repetitive aerosol exposure with *Mtb* drives greater lung damage and cavitation than a single exposure. This suggests that human lung destruction due to TB may be exacerbated in settings where individuals are repeatedly exposed.   MMP1-inhibition with cipemastat did not prevent the development of cavitation in our model.

KEYWORDS: tuberculosis; cavity; matrix metalloproteinase; rabbit; pathogenesis; cipemastat; trocade; collagenas.

BACKGROUND

Tuberculosis is a major cause of morbidity and mortality with 10.4 million new cases of tuberculosis and 1.4 million deaths in 2015 [1]. Individuals with extensive lung disease develop a spectrum of gross lesions including diffuse inflammation, tubercles, caseous tubercles, and cavities. The most consequential of these lesions is the lung cavity.

Cavities are not specific to tuberculosis, but they are the greatest risk factor fortransmission of bacilli [2–5]. Cavitary tuberculosis is also more difficult to treat than non-cavitary tuberculosis and is associated with the emergence of drug-resistance [6]. For patients with cavitary tuberculosis who are cured, the cavities may remain, offering a niche for other opportunistic infections [7]. Cavitary lesions that do resolve are associated with fibrotic scarring and chronically diminished pulmonary function [8,9].

A perfect storm of pathologic features coincide within cavities to drive transmission and a reduced likelihood of treatment success. The interior surface of the cavity wall represents an immune sanctuary that permits high levels of extracellular bacterial proliferation [6,10]. Moreover, cavities often communicate with the conducting airways of the lung, providing a physical conduit for aerosolization and transmission of *Mycobacterium tuberculosis (M. tuberculosis*) bacilli [11]. Finally, diminished vascularity and widespread necrosis within the cavity wall reduces the penetration of chemotherapeutic drugs [12–15].

Despite the importance of cavities to the natural history of tuberculosis, the mechanism of cavity formation in tuberculosis remains unclear. Histologically, cavities are thought to arise from necrotic granulomas, whose centers are both devoid of extracellular matrix. Pulmonary extracellular matrix is composed primarily of collagen and elastin, which provide mechanical support to the lung while maintaining compliance and elasticity. The expression of collagenases leads to caseation, suggesting that matrix depletion may be an early mechanistic driver of cavitation [16–18]. Indeed, increased expression

of collagenases is also associated with cavity formation in both animal models and tuberculosis patients [19,20] .

A limitation to studying tuberculosis cavitation is the lack of reproducible animal models. Mice and guinea pigs rarely develop cavities while they do occur in NHP and rabbit models [21–23]. Previous studies employed pre-sensitization with heat-killed tubercle bacilli together with a high-dose aerosol challenge, transthoracic challenge, or intrabronchial instillation [24–26]. While these methods result in cavitation in some animals, they also generate extensive pneumonitis making it difficult to monitor granuloma formation, necrosis and progression to cavity formation.

Here we describe a novel rabbit model for cavitary tuberculosis based on repetitive aerosol exposure. This model reliably generates multiple cavitary foci in 60 – 80% of study animals in a short period of time. Compared with single exposures of the same total bacterial burden, repetitive exposure generated more advanced disease and more cavitary foci, suggesting that repetitive exposure to aerosolized bacilli may be an important determinant for the severity of tuberculosis in high-incidence settings. Coincidentally, the number of exposures experienced by newly infected TB patients was recently reported as a risk-factor for disease progression [27]. We also confirmed that this model develops human-like tuberculosis cavities where matrix depletion was a pathologic feature of cavity development. Finally, we applied this model to screen cipemastat, a potent inhibitor of MMP-1, as a targeted inhibitor and therapeutic agent to limit tuberculosis cavitation [28,29].

METHODS

Infection of Rabbits: All procedures involving live animals were conducted in accordance with protocols approved by the Institutional Animal Care and Use Committee at the Johns Hopkins University School of Medicine. Female New Zealand White rabbits (2.5 - 3.5 kg) were

purchased from Robinson Services (Mocksville, NC) and housed individually in a BSL-3 facility without cross-ventilation. Rabbits were infected in a Madison aerosol droplet generation chamber (College of Engineering Shops, University of Wisconsin, Madison, WI). The aerosol inoculum for the chamber was prepared by dilution of log-phase bacterial culture of *M. tb* H$_{37}$Rv to the appropriate OD for each experimental group.

Cipemastat dosing: Cipemastat was obtained from the Roche Corporation (Basel, Switzerland) and the identity of the compound was confirmed by LC/MS.

Rabbits in the treatment group were given 100 mg/kg cipemastat orally by body weight adjusted weekly using PediaSure as a vehicle. The concentration of cipemastat in the vehicle was 100 mg/mL. Cipemastat treatment and vehicle shams were administered daily during study weeks 5 through 10.

Pharmacokinetic analysis of cipemastat in plasma: Three rabbits were given a single 100 mg/kg oral dose of cipemastat. Peripheral blood samples were collected every 30 minutes, then at 4, 6, 8, 12, and 24 hours.

Experimental samples were analyzed in tandem with a standard curve prepared in untreated rabbit plasma. Plasma concentrations of cipemastat were detected and quantified by liquid chromatography- tandem mass spectrometry (LC-MS/MS; AB SCIEX QTRAP 5500). Liquid chromatography was carried out by reverse phase gradient elution between 90% mobile phase A (0.1% formic acid in water) to 95% mobile phase B (100% acetonitrile) over 2 minutes on a ZORBAX Eclipse Plus C18 column (2.1 x 50 mm, 3.5 μm, Agilent Technologies, Part No. 9597432-902). Selected ion monitoring of the cipemastat parent ion at m/z 437.2 identified daughter ions at m/z 262.2 and 404.3. These transitions were supported by predicted masses in a cipemastat fragmentation map and agree with transitions identified by Hopfgartner *et al*. (2003) [30].

Cipemastat concentration in eluate was measured as area under the curve for mass transition peaks. Analysis was conducted using Analyst (SCIEX) and companion software MultiQuant (SCIEX). Pharmacokinetics analysis (PK) of total drug exposure over time (AUC_{0-24}), half-life ($T_{1/2}$), concentration maximum (C_{max}) and time of concentration maximum (T_{max}) were calculated using 2 compartment 1st order pharmacokinetics analysis with WinNonlin software (version 7.0, Pharsight Corp).

Computerized tomography scans: Rabbits were imaged using a CereTom 8-slice clinical computerized tomography (CT) scanner with a 32.5 cm bore diameter (NeuroLogica, Boston, MA). To achieve reconstructions in the absence of motion artifact, rabbits underwent breath-holding during CT scans as described by Kübler [31].

Identification of Cavities from CT Reconstructions: CT reconstructions were viewed using VivoQuant software (Invicro). Lung cavities were radiologically identified from CT scan reconstructions as a contiguous set of volume elements (voxels) whose size is defined by the limit-of-resolution of the CT scanner, within the lungs, with densities close to air (-1000 – 910 Hounsfield unit [HU]) and encapsulated by consolidation defined as a continuous region of voxels with densities similar to water (-725 – 1000 HU). This radiological definition was consistent with the consensus definition for cavities advanced by Gadkowski and Stout (2008) [2].

Contiguous airspace and consolidation regions were selected by connected thresholding in the density range for each landmark. Continuity of consolidation around the airspace was confirmed by eye.

Lung extraction and fixation: After 14 weeks, rabbits were sedated and euthanized. Lungs were removed and photographed and then gently infused with intratracheal 10% neutral buffered formalin and fixed for 48 hours.

Quantification of the extent of lung disease: Gross images were obtained using a Nikon D3200 digital camera and a Nikon NIKKOR lens and analyzed with ImageJ to identify the areas of visually diseased lung as a fraction of the total area of splayed lung [32]. This fraction was used as an estimate of the percentage of diseased lung.

Histology and trichrome quantification: Transverse lung slices were collected for paraffin embedding and histologic sectioning. Serial 5 μm sections were stained using hematoxylin and eosin (H&E), Masson's trichrome stain, or the acid-fast stain. Image capture for semi-quantitative trichrome quantification was performed on a Nikon Eclipse 90i microscope with attached Nikon DS-Ri1 color camera, and analyzed using NIS Elements Advanced Research software (Nikon Instruments, Melville, NY). Regions of interest (ROIs) included the full thickenss of the cavity wall while excluding necrotic debris and air space at the cavity interior. Positive staining was calculated as a percentage of the total ROI.

Substrate cleavage assay: Recombinant human MMP-1 (BioVision, Milpitas CA) was added to a solution of type I collagen (Thermo Fisher Scientific, Waltham MA) in PBS at a molar ratio of 1:5. 100 uL Novex Zymogram 1X Developing Buffer (Thermo Fisher Scientific, Waltham MA) with or without 1μg cipemestat was added to this solution prior to incubation at 37° C for 24 hours. At 24hr, an equal volume of EDTA was added to stop the cleavage reaction, and the products were briefly boiled and subjected to SDS-PAGE on a Mini-Protean TGX precast gel (Bio-Rad, Hercules CA).

RESULTS

Repetitive aerosol exposure to *M. tuberculosis* causes a high frequency of cavitation in a rabbit model.

Previous investigations suggested that sensitization with heat-killed Mycobacteria prior to infection increased the frequency and severity of cavitation in rabbit models [26,31]. We reasoned that multiple aerosol challenges with virulent *M. tuberculosis* would provide a robust sustained immune sensitizing effect while simultaneously antagonizing both the innate and adaptive defenses.

To test this hypothesis, we conducted a limited-power study by exposing rabbits to *M. tuberculosis* in two different patterns. For our studies we defined exposure as the product of the bacterial concentration in the aerosol inoculum and the total time spent in the aerosol chamber. One group of rabbits received five aerosol challenges with *M. tuberculosis* at a constant exposure of OD_{600} 0.05 spread evenly over a two week period. A second group of rabbits received a single aerosol challenge with *M. tuberculosis* where the aerosol exposure was OD_{600} 0.25, of five times that of the repetitive exposure (Fig. 1A). These challenges corresponded to an extrapolated day-1 bacterial implantation of 400 CFU per exposure in the OD 0.05 group and 2200 CFU per exposure in the OD 0.25 group (Fig. S1). We confirmed that the cumulative exposure was the same for both groups by measuring the colony-forming units in the aerosol inoculum (Fig. 1A).

To address the possibility that the infection chamber does not achieve aerosol concentrations of bacilli that are linearly correlated with the optical density of the aerosol inoculum, we performed a titration assay to compare the optical density of the aerosol inoculum with the day-1 implantation of bacteria in rabbit lungs, and showed a linear correlation in the optical density range used in these experiments (Fig. S1). Indeed, our data indicate that it is likely that repetitive-exposure rabbits were infected on every occasion of exposure as bacteria were recovered from the lungs of all rabbits in the lowest optical-density exposure group of our chamber titration experiment (Fig. S1).

We monitored rabbits using computer tomography (CT) scans. These data showed that 75% (3 of 4) of the animals in the repetitive exposure group experienced at-least one cavity versus 25% (1 of 4) of the animals in the repetitive exposure group (Fig. 1B). Of those animals that developed cavities, those in the repetitive exposure group showed a trend toward more cavities per animal than those in the single exposure group (Fig. 1C). On week-10 of the experiment, the rabbits were sacrificed and the lungs were fixed. Semi-quantitative gross pathologic analysis showed that rabbits in the repetitive aerosol group experienced worse lung disease than those in the single exposure group (Fig 1D and S2). In light of the limited number of rabbits involved in this study, these data suggest that repetitive exposure caused an increase in the severity of disease as well as the frequency and severity of cavities.

Cavities from repetitive exposure formed quickly, showed dynamic behavior, and often persisted for many weeks.

Focal matrix depletion precedes tuberculosis cavitation, so we sought to define the optimal treatment window for the prevention of cavitation as the weeks before the greatest frequency of cavitation. To study the dynamics of cavity formation generated by repetitive exposure to *M. tuberculosis*, we infected eight rabbits using the repetitive exposure protocol and observed their lungs using CT scans at weeks three, six, eight and 16. The overall frequency of cavitation in this study was 87% (7 of 8), further supporting our previous observations with the repetitive exposure method (Fig. 2A). The greatest increase in the frequency of cavitation occurred between weeks six and eight, during which time the frequency of cavitation among rabbits increased from 11% (1 of 8) at week six to 50% (4 of 8) at week eight (Fig. 2A). Between week eight and week 16, the frequency of cavitation increased modestly to 63% (5 of 8) but was marked by occasional resolution of existing cavities and the generation of new cavities.

Cavity morphology over time was observed by CT scan reconstructions. We used density segmentation analysis to identify cavities as air-filled spaces that were not connected to the bronchial tree. From this analysis, we identified three patterns of change in cavity morphology: (1) cavity growth (Fig. 2B and C, examples 1, 2 and 3) (2) cavity shrinkage (Fig. 2B and C, example 2 and 3), and (3) cavity resolution

(Fig. 2B and C, example 4). Together, these data demonstrate that cavities most-often formed between six and eight weeks after the initial aerosol exposure and were persistent though dynamic structures between weeks eight and 16 of the study.

Histologic observations support the hypothesis that central necrosis and matrix depletion are prerequisites for cavitation.

A large body of historic literature, in addition to our own observations, suggests that tuberculosis cavities arise from necrotic granulomas. Since we had not previously worked with a model that generates cavities by repetitive exposure to *M. tuberculosis*, we investigated whether the pathologic phenotype of lung destruction was similar to human disease. Histology samples collected from rabbits infected by repetitive exposure displayed many of the microscopic findings described in tuberculosis pathology reports (Fig. 3A) [10,21,33,34]. These hallmarks included granulomas, necrotic granulomas and cavities. Histologic observations from the repetitive exposure model show that the cytoarchitecture between necrotic granulomas and cavities was similar, further supporting a close relationship between the two lesions (Fig. 3A-B, 4C).

The cavities generated by repetitive exposure were marked by large proliferations of acid-fast bacteria along their inner surface and a wall enriched with fibrosis (Fig. 3B). Since our investigations are predicated on the pathologic observation that matrix depletion predisposes to cavitation, we also confirmed that collagen matrix depletion was a hallmark of cavitary lesions from repetitive exposure (Fig. 4). These observations show that repetitive aerosol exposure in rabbits generates a spectrum of histologic lesions commonly observed in tuberculosis pathology studies and validates the model for our studies by showing that pathologic matrix depletion is modeled by rabbits following repetitive aerosol infection.

The collagenase MMP-inhibitor cipemastat is orally bioavailable in rabbits and reaches therapeutic concentrations in the peripheral blood.

We previously showed that MMP-1 transcripts accumulated in the areas near *M. tuberculosis*-induced lung damage suggesting that MMP-1 activity might drive tissue destruction in tuberculosis [19]. We hypothesized that if MMP-1 was the major driver of tissue matrix destruction in tuberculosis patients, then inhibiting MMP-1 should prevent cavities (Fig. 3C). Cipemastat is a potent inhibitor of MMP-1 and was originally developed by the Roche Corporation as an anti-arthritis agent [28,29]. We first confirmed that cipemastat did not have intrinsic anti-mycobacterial properties that our stock of cipemastat was able to inhibit MMP-*1 in vitro* (Table S1 and Fig. S4). Next, we conducted a 3-rabbit pharmacokinetic study to confirm that cipemastat was orally bioavailable in rabbits and had suitable kinetics for a daily dosing regimen (Table 1). During the PK study, rabbits were given a single oral dose of cipemastat at a concentration of 100 mg/kg of body weight, a dose that was shown to be within the tolerability and efficacy range in human and animal studies [35,36].

The results of the PK study showed a 24-hour $AUC_{0-24 \text{ hours}}$ of 21.79 h·µg/mL (49.9 µM·h), consistent with previouly published oral dosing studies (Table 1) [35,36]. Importantly, we found that the plasma concentration remained above the publshed IC_{50} of 26 ng/mL (60 nM) for 22 out of 24 hours following a single oral dose (Table 1 and Fig. S3) [28]. These results suggest that cipemastat shows good oral bioavaliability in rabbits and confirms that a daily dosing regimen is sufficient to maintain plasma concentration levels above the IC_{50} during most of a 24 hour period.

Cipemastat monotherapy did not protect against extensive lung destruction and cavitation.

We randomized 17 rabbits into an 8 rabbit vehicle-group and a 10 rabbit cipemastat-group. All rabbits received 1 mL of PediaSure per kilogram of body weight. Rabbits in the cipemastat group received 100 mg/kg of cipemastat in PediaSure, the same dose that was validated during our PK study. Cipemastat was

given orally from study weeks 5 through 10. This treatment window was consistent with the four weeks preceding the maximum frequency of cavitation and the time during which we predict that pathologic lesions will undergo matrix depletion. Our results are based on six control-group rabbits and seven cipemastat-treated rabbits.

During weeks seven, nine, 12 and 14 we performed breath-hold computerized tomography (CT) scans on all study rabbits. These CT scans revealed no difference in the number of cavities or severity of cavitation between the control and treatment groups throughout the study (Fig. 6A, 6B and S5). We did notice a repeated trend toward worse cavitary disease among rabbits in the cipemastat-treated group. The animals were sacrificed during week 14 and the lungs were fixed and scored for disease severity by two independent blinded observers (Fig. 6C). We also quantified the extent of disease within the lungs by cutting the lungs in the transverse plane and reporting the overall percentage of all lung slices with grossly visible disease (Fig. 6C). Neither severity scoring or disease quantification showed a difference between experimental groups.

Collagen content at cavity walls was not changed by cipemastat treatment.

Tuberculosis lung lesions are often encircled by a fibrotic wall [21]. This pathologic matrix deposition is also a feature of rabbits modeling cavitary tuberculosis (Fig. 3B and 6D). Since cipemastat inhibits collagenase activity, we predicted that cipemastat administration should increase the collagen content around tuberculosis lesions. We used hue-thresholding to quantify the amount of collagen identified in blue by applying Masson's trichrome stain to formalin-fixed parafin-embedded lung sections of cavities (Fig. 6D). Using this method we were unable to identify any difference in the collagenous content of cavity walls suggesting that cipemastat treatment did not change the phenotype of pathologic collagen accumulation around cavities in the rabbit model (Fig. 6D).

CONCLUSIONS

We have developed a novel model for cavitary tuberculosis based on repetitive aerosol exposure to virulent *M. tb*. Our data show that repetitive exposure over a two week period produced more advanced disease and more cavities than a single exposure, even when we carefully adjusted the concentrations bacteria in the aerosol inoculum to provide the same total exposure between groups. This finding suggests a link between repetitive exposure and tuberculosis exacerbation and is further supported by recent epidemiological evidence that multiple exposures to infected contacts increases the risk of tuberculosis progression [27]. An association between repetitive exposure and severe tuberculosis may have important implications for epidemiology and infection control in high-incidence regions of the world [37].

Our experiments did not evaluate the mechanism of repetitive-exposure related disease exacerbation; however, it is likely that the driver of more severe disease in repeatedly exposed animals is repeated priming of cell-mediated immunity. Although untested, repetitive exposure may cause a cascading set of T-cell priming and expansion events that disproportionately exacerbate the immune response against *M. tuberculosis* antigen in the lung [38].

Our data show that modeling cavitary tuberculosis by repetitive aerosol exposure also models a spectrum of human lesions and pathologic matrix depletion associated with caseous and cavitary pulmonary tuberculosis [39]. We took advantage of this model to screen cipemistat, a potent and specific MMP-1 inhibitor, as an inhibitor of cavitation [28]. Our study was supported by a molecular phenotype in which MMP-1 expression increased around tuberculous lesions with matrix destruction [19]. In these experiments, we administered cipemistat for four weeks preceding the development of caseous and cavitary lesions in the repetitive aerosol model. However, our results did not show a reduction in cavitation or disease severity.

As part of our investigations, we confirmed that the plasma concentrations of cipemistat were well above the IC_{50} during the 24 hour dosing cycle. We did not sample the concentration of

cipemistat in tuberculosis lesions, therefore it is possible that cipemistat did not reach inhibitory concentrations within granulomas undergoing matrix destruction. Furthermore, MMP activity may be highly localized in pericellular niches [40]. Alternatively, MMP-1 may act in conjunction with other extracellular collagenases to drive matrix depletion and that the inactivation of MMP-1 did not appreciably change the dynamics of cavity formation, reflecting redundancy in the proteolytic cascade. Finally, it is possible that MMP-1 is not a mediator of matrix depletion and cavitation. The increased expression of MMP-1 at tuberculosis lesions may be purely associative or indicate another role for MMP-1 in the pathobiology of tuberculosis.

Our results demonstrate an entirely new system to study tuberculosis cavities. We show that repetitive exposure to aerosolized *M. tuberculosis* produces a pathologically relevant phenotype for screening pre-clinical agents toward the prevention and treatment of cavity formation.

STATEMENT OF AUTHOR CONTRIBUTIONS

MEU   Study design, data collection, data analysis, data interpretation, literature search, generation of figures, writing of manuscript, review and editing of manuscript

EAI   Study design, data collection, data analysis, data interpretation, literature search, generation of figures, writing of manuscript, review and editing of manuscript.

KB   Data analysis, data interpretation, generation of figures, review and editing of manuscript.

AK   Conceptualization of hypotheses, study design, interpretation of data, review and editing of manuscript.

PTE   Conceptualization of hypotheses, study design, data interpretation, review and editing of manuscript.

WRB   Conceptualization of hypotheses, study design, data interpretation, literature search, review and editing of manuscript, resources to support project.

SOURCES

1. WHO | Global tuberculosis report 2016 [Internet]. WHO. [cited 2017 Jul 19]. Available from: http://www.who.int/tb/publications/global_report/en/

2. Gadkowski LB, Stout JE. Cavitary Pulmonary Disease. Clin Microbiol Rev. **2008**; 21(2):305–333.

3. Bailey WC, Gerald LB, Kimerling ME, et al. Predictive Model to Identify Positive Tuberculosis Skin Test Results During Contact Investigations. JAMA. **2002**; 287(8):996–1002.

4. Grosset J. Mycobacterium tuberculosis in the Extracellular Compartment: an Underestimated Adversary. Antimicrob Agents Chemother. **2003**; 47(3):833–836.

5. Yoder MA, Lamichhane G, Bishai WR. Cavitary pulmonary tuberculosis: The Holy Grail of disease transmission. Curr Sci. **2004**; 86(1):74–81.

6. Kaplan G, Post FA, Moreira AL, et al. Mycobacterium tuberculosis growth at the cavity surface: a microenvironment with failed immunity. Infect Immun. **2003**; 71(12):7099–7108.

7. Davies. Aspergilloma and residual tuberculous cavities—the results of a resurvey. Tubercle. **1970**; 51(3):227–245.

8. Chakaya J, Kirenga B, Getahun H. Long term complications after completion of pulmonary tuberculosis treatment: A quest for a public health approach. J Clin Tuberc Mycobact Dis. **2016**; 3:10–12.

9. Singla N, Singla R, Fernandes S, Behera D. Post treatment sequelae of multi-drug resistant tuberculosis patients (PDF Download Available) [Internet]. ResearchGate. [cited 2017 Aug 10]. Available from: https://www.researchgate.net/publication/44599152_Post_treatment_sequelae_of_multi-drug_resistant_tuberculosis_patients

10. Canetti G. The Tubercle Bacillus in the Pulmonary Lesion of Man. 1st ed. Springer Publishing Co.; 1955.

11. Dannenberg AM. Pathogenesis of Human Pulmonary Tuberculosis. ASM Press; 2006.

12. Prideaux B, Via LE, Zimmerman MD, et al. The association between sterilizing activity and drug distribution into tuberculosis lesions. Nat Med. **2015**; .

13. Dartois V. The path of anti-tuberculosis drugs: from blood to lesions to mycobacterial cells. Nat Rev Microbiol. **2014**; 12(3):159–167.

14. Minchinton AI, Tannock IF. Drug penetration in solid tumours. Nat Rev Cancer. **2006**; 6(8):583–592.

15. Datta M, Via LE, Kamoun WS, et al. Anti-vascular endothelial growth factor treatment normalizes tuberculosis granuloma vasculature and improves small molecule delivery. Proc Natl Acad Sci U S A. **2015**; 112(6):1827–1832.

16. Rojas-Espinosa O, Dannenberg AM, Sternberger LA, Tsuda T. The Role of Cathepsin D in the Pathogenesis of Tuberculosis. Am J Pathol. **1974**; 74(1):1–17.

17. Elkington PT, D'Armiento JM, Friedland JS. Tuberculosis Immunopathology: The Neglected Role of Extracellular Matrix Destruction. Sci Transl Med. **2011**; 3(71):71ps6.

18. Al Shammari B, Shiomi T, Tezera L, et al. The Extracellular Matrix Regulates Granuloma Necrosis in Tuberculosis. J Infect Dis. **2015**; 212(3):463–473.

19. Kübler A, Luna B, Larsson C, et al. Mycobacterium tuberculosis dysregulates MMP/TIMP balance to drive rapid cavitation and unrestrained bacterial proliferation. J Pathol. **2015**; 235(3):431–444.

20. Elkington P, Shiomi T, Breen R, et al. MMP-1 drives immunopathology in human tuberculosis and transgenic mice. J Clin Invest. **2011**; 121(5):1827–1833.

21. Leong FJ, editor. A Color Atlas of Comparative Pathology of Pulmonary Tuberculosis.

22. Gupta UD, Katoch VM. Animal models of tuberculosis. Tuberc Edinb Scotl. **2005**; 85(5–6):277–293.

23. Dannenberg AM, Collins FM. Progressive pulmonary tuberculosis is not due to increasing numbers of viable bacilli in rabbits, mice and guinea pigs, but is due to a continuous host response to mycobacterial products. Tuberculosis. **2001**; 81(3):229–242.

24. Yamamura Y, Yasaka S, Yamaguchi M, Endo K, Iwakura H, Nakamura S. Experimental formation of the tuberculous cavity in the rabbit's lung; experimental study on the tuberculous allergy. Kekkaku; 1954.

25. Converse PJ, Dannenberg AM, Estep JE, et al. Cavitary tuberculosis produced in rabbits by aerosolized virulent tubercle bacilli. Infect Immun. **1996**; 64(11):4776–4787.

26. Nedeltchev GG, Raghunand TR, Jassal MS, Lun S, Cheng Q-J, Bishai WR. Extrapulmonary dissemination of Mycobacterium bovis but not Mycobacterium tuberculosis in a bronchoscopic rabbit model of cavitary tuberculosis. Infect Immun. **2009**; 77(2):598–603.

27. Lee RS, Proulx J-F, Menzies D, Behr MA. Progression to tuberculosis disease increases with multiple exposures. Eur Respir J. **2016**; 48(6):1682–1689.

28. Lewis EJ, Bishop J, Bottomley KM, et al. Ro 32-3555, an orally active collagenase inhibitor, prevents cartilage breakdown in vitro and in vivo. Br J Pharmacol. **1997**; 121(3):540–546.

29. Brewster M, Lewis JE, Wilson KL, Greenham AK, Bottomley KMK. Ro 32-3555, an orally active collagenase selective inhibitor, prevents structural damage in the STR/ORT mouse model of osteoarthritis. Arthritis Rheum. **1998**; 41(9):1639–1644.

30. Hopfgartner G, Husser C, Zell M. Rapid screening and characterization of drug metabolites using a new quadrupole-linear ion trap mass spectrometer. J Mass Spectrom JMS. **2003**; 38(2):138–150.

31. Kubler A. Development and Investigation of a Rabbit Model of Tuberculosis Tissue Destruction. [London, United Kingdom]: Imperial College London; 2013.

32. J Schindelin, Arganda-Carreras, Frise. Fiji: an open-source platform for biological-image analysis.

33. Rich A. The Pathogenesis of Tuberculosis. 1st ed. Baltimore, Maryland: Charles C Thomas; 1944.

34. Rom WN, Garay SM. Tuberculosis. 2nd ed. Philadelphia: Lippincott Williams & Wilkins; 2004.

35. Hemmings FJ, Farhan M, Rowland J, Banken L, Jain R. Tolerability and pharmacokinetics of the collagenase-selective inhibitor Trocade in patients with rheumatoid arthritis. Rheumatol Oxf Engl. **2001**; 40(5):537–543.

36. Ishikawa T, Nishigaki F, Miyata S, et al. Prevention of progressive joint destruction in collagen-induced arthritis in rats by a novel matrix metalloproteinase inhibitor, FR255031. Br J Pharmacol. **2005**; 144(1):133–143.

37. Nardell E, Churchyard G. What is thwarting tuberculosis prevention in high-burden settings? N Engl J Med. **2011**; 365(1):79–81.

38. Behar SM, Carpenter SM, Booty MG, Barber DL, Jayaraman P. Orchestration of pulmonary T cell immunity during Mycobacterium tuberculosis infection: immunity interruptus. Semin Immunol. **2014**; 26(6):559–577.

39. Tomashefski JF, editor. Dail and Hammar's Pulmonary Pathology. 3rd ed. Springer Publishing Co.; 2008.

40. Murphy G, Nagase H. Localizing matrix metalloproteinase activities in the pericellular environment. FEBS J. **2011**; 278(1):2–15.

TABLES

Table 1. Pharmacokinetic data for cipemastat following bolus dosing in rabbit plasma.

		parameter		
drug	$\mathbf{AUC_{0\text{-}24}}$ **(hr*μg/mL)**	$\mathbf{C_{max}}$ **(μg/mL)**	$\mathbf{T_{max}}$ **(hr)**	$\mathbf{T_{1/2}}$ **(hr)**
cipemastat	19.92 (16.42-23.44)	3.02 (1.99-4.44)	2.47 (1.98-3.07)	1.87 (1.22-2.23)

FIGURES

Figure 1. Infection parameters and disease patterns for rabbits challenged in the single and repetitive exposure groups. (A) Experimental exposure conditions and timing. Single exposure group rabbits received a single implantation with approximately 2500 bacteria on day 8 and sham exposures on days 1, 4, 12 and 16. Repetitive exposure group rabbits received five repetitive exposures resulting in implantation of approximately 500 bacteria on each of days 1, 4, 8, 12 and 16. Exposure was calculated based on the CFU in the aerosol inoculum. The repetitive exposure was calculated as the sum of the CFU/mL on each day of infection. (B) Frequency of cavitation among rabbits in the single and repetitive exposure groups. (C) The number of cavities per animal in the single and repetitive exposure groups. Cavity counts are only plotted for the animals that demonstrated cavitation. (D) Quantification of the fraction of lung identified as diseased by gross observation for rabbits in the single exposure and repetitive exposure groups.

Figure 2. Timing of cavitation and cavity growth dynamics in the repetitive aerosol method. (A) The frequency of cavitation mapped to time after start of infection. The solid line indicates the cumulative frequency of cavitation among the cohort of 9 rabbits. The dashed line indicates the frequency of cavitation among the cohort at the specific time point and is distinguished from the solid line by the occurrence of cavity resolution. (B) Cavity volume mapped to time after the start of infection for four representative cavities demonstrating (1) continuous growth, (2, 3) growth and shrinking behavior, and (4) growth and resolution. Cavities were identified as lung volumes not connected to the normal bronchial structure with densities between -875 and -1024 Hounsfield units and points on the x-axis indicating a non-cavitary focus are plotted at the limit-

of-resolution for the CT scanner. The y-axis is plotted using a logarithmic base 3 scale since measured volume varies closely as the cube of the radius of a spheroid object so that relationship among cavity volumes are more comparable to the two-dimensional reconstructions in C. (C) Transverse CT-scan reconstructions showing each of the foci identified in B.

Figure 3. Histologic patterns of tuberculosis lesions in rabbits infected by repetitive aerosol exposure. (A) Representative H&E demonstrating lesions commonly observed in rabbits infected by repetitive aerosol exposure. (B) Serial sections from the boxed region demarcated in A stained with hematoxylin and eosine, acid-fast bacilli, and Masson's trichrome stain. Masson's trichrome identifies collagen in blue hues. (C) Overview of the model for collagenase mediated destruction of extracellular matrix in proximity to a cavity.

Figure 4. Collagen enrichment in lung lesions from rabbits infected with *Mycobacterium tuberculosis*. (A) Examples of H&E stained tissue fields used for quantification of collagen enrichment analysis. Black rectangles represent example high-resolution fields used for quantification in B and traces in C. Arrow-heads indicate examples of the histologic regions surveyed during the relative collagen quantification reported in 4B. (B) Relative enrichment in collagen identified by blue hues in the Masson's trichrome stain. Surveys of collagen enrichment were random in normal appearing lung tissue and from regions 500 μm in length at the centers of lesion fields in granulomas and necrotic granulomas. Surveys of collagen enrichment from the cavity edge were defined as regions within 150 μm of the cavity edge. Multiple surveys were taken from non-overlapping areas within each region and the number above each category indicates the number of unique lesions surveyed. (C) Relative tissue density (grey line, right y-axis) and collagen density (black line, left y-axis) along linear traces crossing two granulomas,

two necrotic granulomas, and two cavities. All traces are set to the same x and y scale and the minor hash marks in the lowest plot show the regular pattern of surveys continued along each lesion. Dotted lines indicate cavity space on histology.

Figure 5. Experimental overview to investigate the pharmacologic inhibition of tissue destruction and cavitation using cipemastat in rabbits infected with *Mycobacterium tuberculosis*. The predicated temporal window for cavitation was designed based on data presented in figure 2.

Figure 6. The extent of disease severity and cavitation in cipemastat treated rabbits. (A) Average number of cavities per animal for weeks 7, 9, 12 and 14. (B) Average volume of the lung identified as cavity volume by CT-scan and segmentation analysis for weeks 7, 9, 12 and 14. (C) Disease severity scores of lungs assigned subjectively by two independent blinded observers and quantified as the fraction of lung identified as disease in transversely splayed lungs. (D) Quantification of collagen accumulation at the walls of cavities in *M. tuberculosis*-infected rabbits. The example of a cavity wall shows regions identified as collagen.
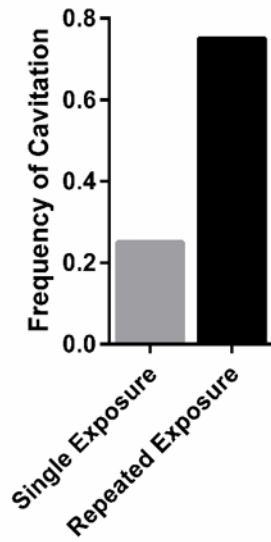
Figure 1.

Figure 2.

Figure 3.

A.

normal lung   large granuloma   necrotic granuloma   cavity

B.

H&E

AFB

Masson's Trichrome

C.

— extracellular matrix   pneumocyte   monocytic and granulocytic leukocytes.   necrotic debris

✂ extracellular collagenases   bronchial/bronchiolar epithelial cells   lymphocytes

bronchus/bronchiole

cavity

Figure 4.

A.

B.

C.

Figure 5.

Figure 6.